Research on the Antitumor Activity and Mechanism of Gramicidin-S

Fengcai Ma, Yang Wan*
Jiangxi University of Traditional Chinese Medicine, Nanchang 330004, Jiangxi, China

Abstract: Lung cancer is a malignant tumor with high morbidity and mortality worldwide, and traditional chemotherapeutic drugs such as platinum drugs (PT) and 5-fluorouracil (5-FU) are limited in their applications by drug resistance and toxic side effects, so there is an urgent need to develop new antitumor drugs that are low-toxicity, precisely targeted, and not easy to be drug-resistant. In this study, we used peptide solid-phase synthesis method to prepare Gramicidin-S (GS). We analyzed the differences in the effects of GS with PT and 5-FU through antitumor activity assay, plasma membrane depolarization assay, and scanning electron microscopy observation of cellular morphology. The results showed that GS significantly reduced A549 cell survival and rapidly induced plasma membrane depolarization, and SEM observation revealed that GS treatment severely damaged A549 cell membranes; whereas, PT and 5-FU had almost no depolarizing effect and weakly damaged cell membranes. The conclusions indicate that GS has potent cell membrane targeting on A549 lung cancer cells and exerts anti-tumor effects by destroying the cytoplasmic membrane, which provides a new direction for the research and development of targeted therapeutic drugs for lung cancer.

***Keywords*:** Gramicidin-S; solid-phase synthesis; A549 cells; platinum drugs; 5-fluorouracil; antitumor activity; plasma membrane depolarization; scanning electron microscopy

1. Introduction

Currently, chemotherapy remains the primary treatment for lung cancer. Commonly utilized chemotherapy agents, including platinum-based compounds and 5-fluorouracil, exhibit limitations such as inadequate targeting, tumor cell drug resistance, and nephrotoxicity, which hinder their effectiveness in clinical settings[1]-[4]. Recently, peptide drugs have emerged as a focal point in the research and development of anti-tumor therapies, owing to their advantages of enhanced targeting, reduced toxicity and side effects, and ease of precise modification[5-8]. Antimicrobial peptides demonstrate both antibacterial and anti-tumor properties. Their mechanisms of action involve disrupting tumor cell membranes and inducing apoptosis, among other[9]. Gramicidin-S (GS), a cyclic antimicrobial peptide consisting of 10 amino acids, has shown preliminary evidence of anti-tumor activity through its analogues[10]. This study aims to synthesize GS using solid-phase methods and systematically assess its anti-tumor activity and mechanisms of action against A549 lung cancer cells, with the goal of providing new insights for the structural optimization and mechanistic research of cyclic peptide anti-tumor agents[11 -[13].

2. Materials and Methods

2.1 Experimental materials

Human non-small cell lung cancer A549 cell line was routinely cultured in RPMI-1640 medium containing 10% fetal bovine serum at 37℃ with 5% CO_2. Fmoc-Pro-(2-CTC)-resin (1% crosslinked, 100-200 mesh, 0.476 mmol/g) was sourced from GL Biochem (Shanghai). Platinum(PT) and 5-fluorouracil (5-FU) were purchased from Sigma Company. All solvents and reagents were used as received.

2.2 Gramicidin S synthesis

Using Fmoc-Pro-(2-CTC)-resin as the solid-phase carrier, swell the resin and perform Fmoc deprotection with 20% piperidine. Add Fmoc-protected amino acids, HBTU, HOBT, and DIEA, then shake for 2 hours. After completing amino acid condensation, repeat the deprotection and condensation steps to synthesize the linear peptide chain. First, cleave the linear peptide from the resin using 1% TFA/DCM. Next, perform a cyclization reaction on the linear peptide to form a cyclic peptide structure. Then, remove the side-chain protecting groups with 95% TFA/H_2O. Precipitate the crude cyclic peptide with cold diethyl ether. Subsequent purification yielded the target peptide GS.

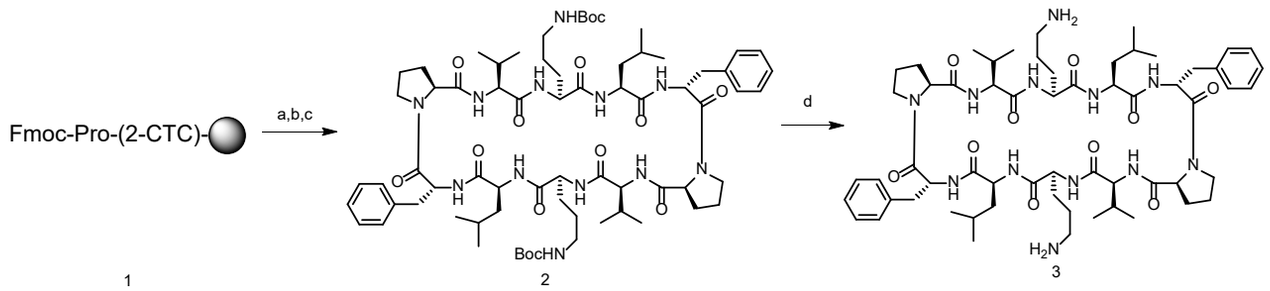

Figure 1. Synthesis of GS. Synthetic conditions: (a) Sequential coupling (Xaa, HBTU,HOBT, DiPEA, DMF) and deprotection (20% piperidine/ DMF, v/v) steps; (b) 1% TFA/DCM, v/v, 5 x10 min; (c) PyBOP, HOBt, DiPEA, DMF; (d) 90% TFA/water, v/v, 25% yield for 3

2.3 Antitumor Activity Assay

A549 cells in the logarithmic growth phase were seeded in 96-well plates, with 100 μL of complete medium added to each well. The cells were cultured adherently in a 37 °C, 5% CO_2 incubator for 24 hours. The drugs GS, PT, and 5-FU were dissolved in DMSO to prepare high-concentration stock solutions. A half-dilution method was employed to generate various drug concentrations. After aspirating the culture medium from the 96-well plate using a pipette, 100 μL of the prepared solution was added to each well. A 20% DMSO medium served as the positive control, while 1640 medium was used as the negative control. Three duplicate wells were included for each concentration level, and the plates were incubated in a 37 °C constant temperature CO_2 incubator for 48 hours. Subsequently, 10 μL of CCK-8 solution was added to each well, followed by a 4-hour incubation. The absorbance (OD value) at 450 nm was measured using an enzyme-linked immunosorbent assay (ELISA) reader to determine the number of viable cells. The percentage of cell viability was calculated according to the specified formula. Data processing software GraphPad Prism was utilized to generate the average curve graph and calculate IC_{50}.

2.4 Polarization-depolarization experiment of the plasma membrane

In this experiment, the DiSC3-5 fluorescence probe method was employed to assess the plasma membrane depolarization effect in A549 cells. Following the culture of A549 cells to the logarithmic growth phase, the cells were centrifuged in HEPES buffer (5 mM HEPES, 20 mM glucose, pH 7.4), washed three times, and subsequently diluted. A total of 1.95 mL of HEPES buffer containing the cells was combined with 0.05 mL of KCl to achieve a final concentration of 0.1 mmol/L, thereby equilibrating the cytoplasmic and external K+ concentrations. The excitation wavelength was set at 622 nm, while the emission wavelength was 670 nm. DiSC3-5 was then added to facilitate the adsorption of fluorescence onto the cell membrane. After observing a decrease in fluorescence intensity that stabilized, GS-1 and GS-2 were introduced at final concentrations of 10 μmol/L, 5-FU at 200 μmol/L, PT-1 and PT-2 at 50 μmol/L, and PT at 100 μmol/L, respectively. Additionally, a 0.9% NaCl buffer group and a blank buffer control group were established. The changes in fluorescence intensity (au) were monitored in real time over a period of 10 minutes to reflect the dynamic trends in plasma membrane potential.

2.5 Scanning Electron Microscopy (SEM) Assay

A549 cells were cultured until they reached the logarithmic growth phase. Following centrifugation, the cell suspension was prepared by washing the cells three times with 0.2 mol/L PBS buffer at pH 7.4. The cells were treated with PT, 5-FU, and GS, while a blank control group without drugs was also established. The samples were incubated at 37°C for 1 hour, followed by centrifugation with PBS buffer and three additional washes. Subsequently, 300 μL of 2.5% glutaraldehyde was added, mixed thoroughly, and the samples were fixed overnight at 4°C. After fixation, the samples were centrifuged and washed three times with 0.2 mol/L PBS buffer to eliminate excess liquid. The washed samples underwent gradient dehydration in ethanol, were incubated in a 4°C refrigerator for 15 minutes, and then centrifuged for another 15 minutes. The dehydrated samples were evenly dispersed in anhydrous ethanol, and 10 μL was placed onto a slide, which was dried using an alcohol lamp. The surface was then gold-coated for 30 seconds, and the morphological changes of the cells were observed using a scanning electron microscope.

3. Results and Discussion

3.1 Synthesis Experiments

GS >95% purity, 13 mg, 11.5% overall yield from SPPS. MS (ESI+): m/z calcd for $C_{60}H_{93}N_{12}O_{10}^{+}$: 1141.71 $[M+H]^{+}$;

found: 1141.42. calcd for 1/2 x $C_{60}H_{93}N_{12}O_{10}^{+}$: 571.36 1/2 $[M+2H]^{2+}$; found: 571.33. The correctness of the products was confirmed.

3.2 Antitumor Activity Assay

We observed that GS, PT, and 5-FU all had tumor cell killing ability(Figure 2), the three drugs had no significant effect on cell survival at low concentrations; cell survival decreased significantly at concentrations ≥10 μM, with GS having the strongest inhibitory effect, and the cell viability had plummeted to less than 10% at 10 μM, showed the strong tumor cell killing ability; PT was the second highest, with the cell viability in the range of 10-100 μM decreasing from about 90% to about 30%; the cytotoxicity of 5-FU changed relatively gently, with the cell viability at 100 μM still > 50%, and a significant decrease in the viability was only observed at a high concentration (>100 μM). From the IC50 trend, the IC_{50} ranking was GS < PT < 5-FU, indicating that the antitumor activity of GS on A549 lung cancer cells was significantly better than that of PT and 5-FU, and that GS may be a potential therapeutic candidate for lung cancer. This result is consistent with the findings of Hu et al[14]. It is hypothesized that the high activity of GS stems from the high affinity of its cyclic structure to the tumor cell membrane, whereas PT and 5-FU act on intracellular targets and are susceptible to drug-resistance mechanisms, and thus have weaker antitumor activity than GS.

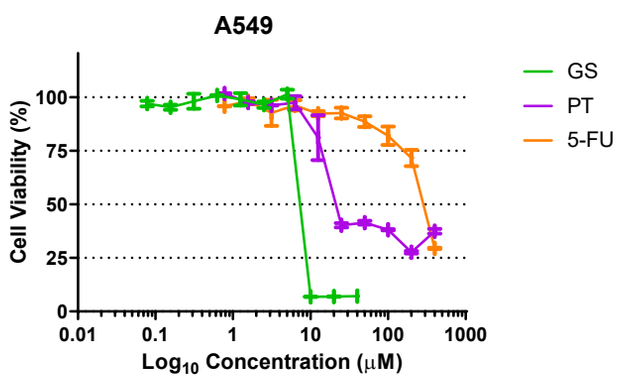

Figure 2. Cytotoxicity assay Results of GS, PT and 5-FU on A549 Cells manner

3.3 Experimental evaluation of plasma membrane depolarization

As illustrated in Figure 3, the fluorescence intensity in the GS-1 (10 μmol/L) and GS-2 (10 μmol/L) treatment groups exhibited a continuous increase over 10 minutes. The fluorescence value for the GS-1 group approached 40 au at the 10-minute mark, indicating that GS compounds significantly induce depolarization of the plasma membrane in A549 cells at this concentration. In contrast, the fluorescence intensities of the 5-FU (200 μmol/L), PT-1 (50 μmol/L), PT-2 (50 μmol/L), and PT (100 μmol/L) treatment groups fluctuated around 0 au, demonstrating no significant trend. The patterns observed in these groups were comparable to those of the 0.9% NaCl buffer and blank control groups, suggesting that these drugs do not elicit a notable depolarization effect on the plasma membrane of A549 cells at the tested concentrations. Therefore, it can be concluded that GS series compounds may induce changes in membrane potential by disrupting the ionic balance of the cell membrane, whereas the mechanisms of action for 5-FU and PT do not rely on the plasma membrane depolarization pathway[15].

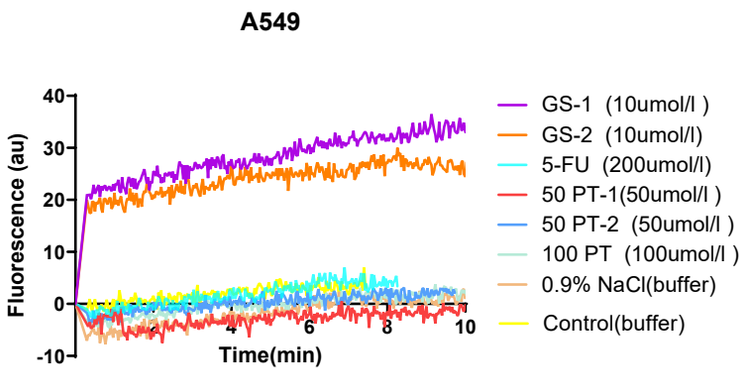

Figure 3. Study on Depolarization of Plasma Membrane of GS, PT and 5-FU

3.4 Scanning Electron Microscopy (SEM) Assay

The A549 cells in the control group exhibit intact morphology, a smooth surface, and characteristic epithelioid cell features (Figure 4). In the PT treatment group, a reduction in cell volume was observed, accompanied by surface wrinkles and a decrease in microvilli. The 5-FU treatment group displayed more pronounced morphological changes, including the emergence of depressions on the cell surface. In contrast, cells in the GS treatment group exhibited significant rupture and collapse, with evident damage to the cell membrane structure, resulting in the loss of cellular integrity. These findings further substantiate that GS primarily exerts its anti-tumor effects by disrupting cell membrane architecture. Both PT and 5-FU demonstrate a relatively weak damaging effect on the A549 cell membrane. GS films exhibit strong targeting capabilities, rapidly breaching the tumor cell barrier and showing resistance to drug tolerance, thereby offering innovative approaches for lung cancer chemotherapy and holding promise for the development of low-toxicity anti-tumor agents.

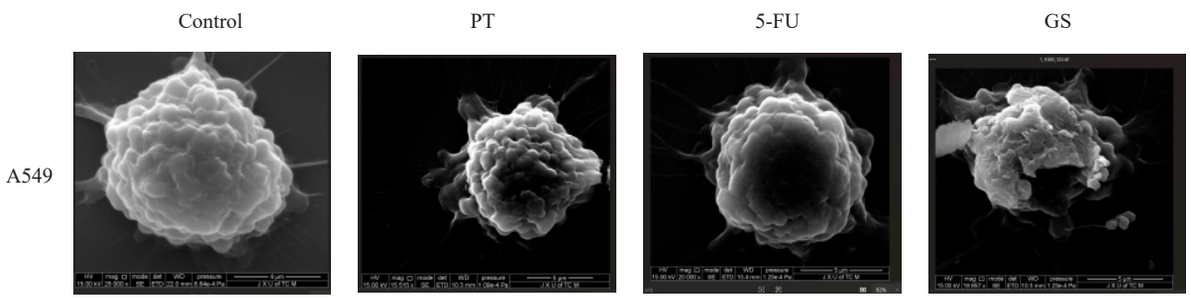

Figure 4. Experimental results of Scanning electron microscopy (SEM)

4. Conclusion

In summary, we have confirmed the anti-tumor effects and mechanisms of GS on A549 cells. GS significantly inhibits the survival rate of A549 cells, demonstrating a much stronger anti-tumor effect compared to PT and 5-FU. GS rapidly induces plasma membrane depolarization and disrupts the structural integrity of the cell membrane. In contrast, PT and 5-FU exhibit minimal plasma membrane depolarization and have a limited damaging effect on the cell membrane. This suggests that the mechanism of action of GS is closely associated with the disruption of ionic balance within the cell membrane, leading to significant alterations in cell morphology and consequent anti-tumor effects. As a polypeptide molecule, GS possesses membrane-targeting capabilities and a unique mechanism for membrane disruption. This mechanism differs from those of traditional chemotherapy agents and is less likely to induce drug resistance. Consequently, GS presents a novel strategy for lung cancer chemotherapy and provides experimental evidence for the structural optimization and development of low-toxicity, membrane-targeted anti-tumor polypeptide drugs. Future research will focus on the in vivo anti-tumor activity and safety of GS in animal models to facilitate its translation into clinical applications.

Acknowledgments

This work was financially supported by the National Natural Science Foundation of China (No. 22577044, 22307049).

References

[1] Liu H, Zou J, Li X, et al. Drug delivery for platinum therapeutics. Journal of controlled release: official journal of the Controlled Release Society,2025,380: 503-523.
[2] Leiter A, Veluswamy R R, Wisnivesky J P. The global burden of lung cancer: current status and future trends. Nature reviews Clinical oncology, 2023, 20(9): 624-639.
[3] Min H Y, Lee H Y. Mechanisms of resistance to chemotherapy in non-small cell lung cancer. Archives of pharmacal research, 2021, 44(2): 146-164.
[4] Siegel R L, Miller K D, Wagle N S, et al. Cancer statistics, 2023. CA: a cancer journal for clinicians, 2023, 73(1): 17-48.
[5] Guan Q, Huang S, Jin Y, et al. Recent Advances in the Exploration of Therapeutic Analogues of Gramicidin S, an Old but Still Potent Antimicrobial Peptide. Journal of medicinal chemistry,2019,62(17):7603-7617.
[6] Chai, Y. Yu, Can. Chen, Z.; Duan, W. Chen, H. Qiu, X.; Xu, Z. Liu, S. Danilenko, A. Frison, G. Alezra, V. Miclet, E. Li, Xiang. Wan, Y. Rapid C-S+ Bond Cleavage via 1,6-Benzyl Elimination for Traceless Modification of Bioactive Peptides. J. Am. Chem. Soc. 2025, 147, 20807−20818.

[7] Zeng, Z. Zhu, J. Deng, X. Chen, H. Jin, Y. Miclet, E. Alezra, V. Wan, Y. Customized Reversible Stapling for Selective Delivery of Bioactive Peptides. J. Am. Chem. Soc. 2022, 144 (51), 23614–23621.
[8] He, F. Chai, Y. Zeng, Z. Lu, F. Chen, H. Zhu, J. Fang, Y. Cheng, K. Miclet, E. Alezra, V. Wan, Y. Rapid Formation of Intramolecular Disulfide Bridges Using Light: An Efficient Method to Control the Conformation and Function of Bioactive Peptides. J. Am. Chem. Soc. 2023,145,22639−22648.
[9] Chauhan Sonia, Dhawan Devinder K, Saini Avneet, et al. Antimicrobial peptides against colorectal cancer-a focused review. Pharmacological Research, 2021, 167(5): 105529.
[10] Guan Q, Chen K, Chen Q, et al. Development of Therapeutic Gramicidin S Analogues Bearing Plastic β, γ-Diamino Acids. ChemMedChem, 2020, 15(12): 1089-1100.
[11] Behrendt R, White P, Offer J. Advances in Fmoc solid-phase peptide synthesis. Journal of Peptide Science, 2016, 22(1): 4-27.
[12] Chen Y L, Lin S Z, Chang J Y, et al. In vitro and in vivo studies of a novel potential anticancer agent of isochaihulactone on human lung cancer A549 cells. Biochemical Pharmacology, 2006, 72(3): 308-319.
[13] Wan Y, Stanovych A, Gori D, et al. β, γ-diamino acids as building blocks for new analogues of Gramicidin S: Synthesis and biological activity. European journal of medicinal chemistry, 2018, 149: 122-128.
[14] Hu C, Wen Q, Huang S, et al. Gramicidin-S-Inspired Cyclopeptidomimetics as Potent Membrane-Active Bactericidal Agents with Therapeutic Potential. ChemMedChem, 2021, 16(2): 368-376.
[15] Baxter A A, Lay F T, Poon I K H, et al. Tumor cell membrane-targeting cationic antimicrobial peptides: novel insights into mechanisms of action and therapeutic prospects. Cellular and Molecular Life Sciences, 2017, 74(20): 3809-3825.